Ionization propensity and electron momentum distribution of the toluene S_1 excited state studied by time-resolved binary $(e,2e)$ spectroscopy

Masakazu Yamazaki,[1] Yaguo Tang,[1,2] and Masahiko Takahashi[1,*]

[1]*Institute of Multidisciplinary Research for Advanced Materials, Tohoku University, Sendai 980-8577, Japan*

[2]*Hefei National Laboratory for Physical Sciences at the Microscale and Synergetic Innovation Center of Quantum Information and Quantum Physics, University of Science and Technology of China, Hefei 230026, China*

(Received 12 August 2016; published 22 November 2016)

We report a time-resolved electron momentum spectroscopy (TREMS) study on the toluene molecule in its S_1 excited state. The toluene S_1 state was prepared by a 267-nm pump laser and probed with a train of 1.2-keV incident electron beam pulses, each having 1-ps temporal width. It is shown through comparisons with molecular calculations that TREMS has an inherent capability to observe spatial distributions, in momentum space, of not only the outermost orbital but also all other, more tightly bound orbitals of a molecular excited state.

DOI: 10.1103/PhysRevA.94.052509

It has long been known that molecular excited states are of importance in many chemical processes in terms of both fundamental and applied research. This is largely because not only are molecular excited states much more reactive than their ground state, but their other chemical properties are also often drastically changed [1]. Furthermore, it is generally accepted that what determines such properties is the spatial distribution of a particular molecular orbital [2]. One may therefore desire to have an experimental method that observes individual electron orbitals of a molecular excited state. However, all of the orbital imaging methods developed so far [3–10] had been hampered in extending the use of the technique for molecular excited states due mainly to their transient nature.

In order to make a breakthrough in the limitation mentioned above, we have recently developed an advanced form of electron momentum spectroscopy (EMS), which is called time-resolved EMS (TREMS) and employs femtosecond laser and picosecond electron pulses in a pump-probe scheme. Basically, EMS is a sort of $(e,2e)$ spectroscopy and involves coincident detection of the two outgoing electrons produced by impact ionization of a continuous beam of electrons having 1 keV or higher energy at large momentum transfer, so it enables one to look at individual molecular orbitals in momentum space [3–6]. However, application of EMS had been limited to studies on targets in their ground state, just as in the case of other orbital imaging methods [7–10]. The exception to this was the pioneering work of Zheng *et al.* [11] on excited sodium atoms prepared by using a continuous-wave ring dye laser. TREMS has been designed to overcome the difficulty of observing electron orbitals of short-lived molecular excited states, by replacing the continuous incident electron beam with electron pulses having a temporal width of 1 ps [12].

A TREMS experiment was reported in [13] for the deuterated acetone molecule in its second excited singlet $S_2(n,3s)$ state with a lifetime of 13.5 ps [14]. On the one hand, this work demonstrated that EMS experiments on short-lived transient species are feasible, opening the door to time-resolved orbital imaging [15,16]. On the other hand, its observation was limited only to the energetically well-separated outermost orbital of the acetone S_2 state. This limitation was due to the fact that the acetone S_2 state rapidly decays into the two CD_3 radicals and one CO molecule through a three-body dissociation process [14]. It was also due to the fact that the poor time resolution (± 35 ps), being almost entirely governed by the group-velocity mismatch between the pump laser and the probe electron beam, was used to have a workable coincidence count rate [13]. In other words, because of the lack of a time resolution fine enough to focus on the acetone S_2 state, the experiment on the higher-binding-energy region had to be affected by the following decay process. Clearly, the potential capability of TREMS to observe individual orbitals of a molecular excited state may have to be examined.

In this paper we report a TREMS experiment in which the toluene molecule in the $S_1(\pi,\pi^*)$ excited state was chosen as the target. The reason for this choice is that the toluene S_1 state has a lifetime of 86 ns [17], much longer than the experimental time resolution of ± 35 ps. Hence, a TREMS experiment without any contributions of the following intramolecular relaxation processes [18] can be made for the toluene S_1 state while the whole valence electronic structure is covered. Here $(e,2e)$ binding energy spectra and a spherically averaged electron momentum distribution measured for the toluene S_1 state are presented and compared with associated molecular calculations at a high level.

The experiment on the toluene S_1 state was carried out using the TREMS apparatus [12]. Briefly, the 800-nm output of a 5-kHz Ti:sapphire femtosecond laser (< 120 fs, 0.8 mJ) was frequency tripled and split into a pump path and an electron-generation path. Most of the 267-nm output power was devoted to the pump path and it was subsequently used as the pump laser (~ 16 μJ) to excite a toluene molecule in a target gas beam to the S_1 state, after the 5-kHz repetition rate was halved by an optical chopper. The remaining portion of the 267-nm output was used in the electron-generation path to yield a train of 267-nm laser pulses by using half-wave plates and polarizing beam splitters, after being attenuated as required. The laser pulse train was then directed toward a back-illuminated photocathode, which was negatively biased to accelerate electron pulses produced via the photoelectric effect up to 1.2 keV. In this way, the laser pulse train was converted to a train of 1.2-keV incident electron beam pulses of 2-mm diameter and 1-ps temporal width with interpulse spacing of 0.2 ns. Here the number of electron pulses in

*Corresponding author: masahiko@tagen.tohoku.ac.jp

one train was set to be either 4 or 8, as discussed later. The resulting pulsed electron beam (∼100 or 200 pA) was then used to induce EMS events, which were recorded by an EMS spectrometer equipped with a spherical analyzer of 220-mm mean radius.

For the EMS measurements, the symmetric noncoplanar geometry was employed, in which two outgoing electrons having equal energies and making equal scattering angles ($\theta_1 = \theta_2 = 45^\circ$) with respect to the incident electron beam axis were detected in coincidence. The binding energy $E_{\rm bind}$ and momentum ($\boldsymbol{p}$) of the target electron, before ionization, can be determined through the following energy and momentum conservation laws [3–6]:

$$E_{\rm bind} = E_0 - E_1 - E_2, \tag{1}$$

$$\boldsymbol{p} = \boldsymbol{p}_1 + \boldsymbol{p}_2 - \boldsymbol{p}_0. \tag{2}$$

Here E_j and $\boldsymbol{p}_j (j = 0,1,2)$ are kinetic energies and momenta of the incident, inelastically scattered, and ejected electrons, respectively. In this kinematic scheme, the magnitude of the target electron momentum p is given by

$$p = \sqrt{(p_0 - \sqrt{2}p_1)^2 + [\sqrt{2}p_1 \sin(\Delta\phi/2)]^2}, \tag{3}$$

with $\Delta\phi$ being the out-of-plane azimuthal angle difference between the two outgoing electrons detected.

The TREMS measurements for the toluene S_1 state were carried out by setting the delay time between the arrival of the pump laser pulse and the probe electron pulse train to be approximately 6 ns, while accumulating data at an ambient sample gas pressure of 1.0×10^{-4} Pa for a 47-day runtime. The energy and momentum resolution were 5-eV full width at half maximum and 0.5 a.u. at $\Delta\phi = 0^\circ$, respectively. Here two types of incident electron beams having four and eight pulses in one train, mentioned earlier, were employed in turn and their results were compared to each other. Use of such a multiple-pulse train is justified in this experiment, because the entire width of the train is much smaller in both cases (0.6 and 1.4 ns) than the 86-ns lifetime of the toluene S_1 state [17]. Furthermore, it can work to increase the incident electron beam intensity and hence the TREMS signal count rate, compared to the single pulse case, while maintaining the moderate energy spread and temporal width of the incident electron beam that are significantly broadened due to space charge effects with the increase in the number of electrons in one pulse [19]. The experiments using the two types of incident electron beams were confirmed to provide essentially the same results and the TREMS experimental data were obtained by summing those accordingly. In addition, it should be noted that since the 5-kHz repetition rate was halved only for the pump laser, the TREMS experiments concurrently produced two kinds of EMS data sets. One is data that were measured with the pump laser (laser-on spectrum). The other is reference data that were measured without the pump laser (laser-off spectrum) and hence they are equivalent to traditional EMS data for the ground-state molecule.

Figures 1(a) and 1(b) show TREMS binding energy spectra thus obtained for the toluene S_0 (ground) and S_1 (excited) states, respectively. The former is the laser-off spectrum

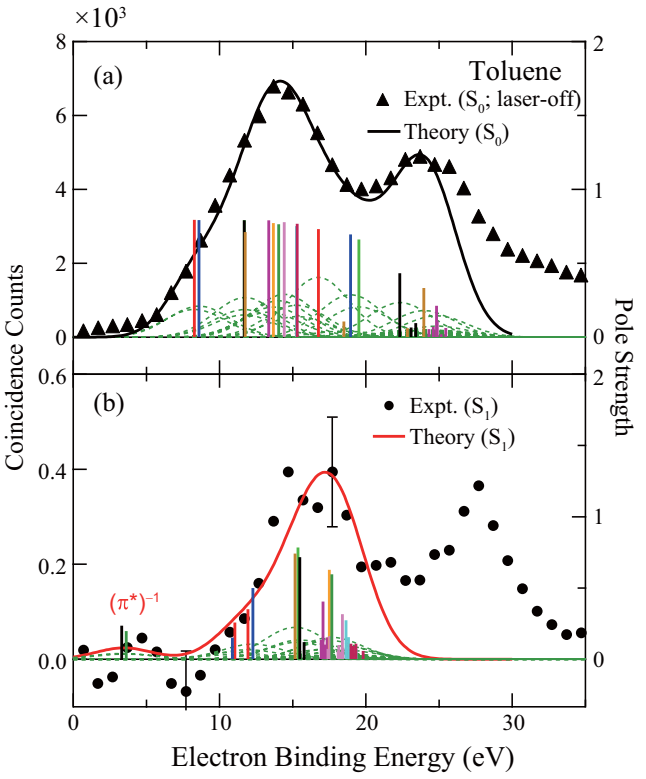

FIG. 1. Comparisons of binding energy spectra between the experiments and SACCI calculations for the (a) S_0 and (b) S_1 states. The dashed lines show the contribution of each transition and the solid line is their sum. Vertical bars represent pole strengths (> 0.05).

itself, which was constructed by plotting the number of true coincidence events summed up over the entire covered $\Delta\phi$-angle range as a function of $E_{\rm bind}$. The latter was generated by subtracting the laser-off spectrum with a weight factor of 0.95 [13] from the laser-on spectrum (though not depicted). Note here that the weight factor was chosen so as to be the maximum value under constraint that the resulting TREMS spectrum should not exhibit an intensity less than zero beyond the experimental error bars. Also included in the figures are associated theoretical spectra, which were created in the following manner: The most widely used scattering model for EMS is the plane-wave impulse approximation [3–6] that describes EMS cross sections as

$$\frac{d^3\sigma_{\rm PWIA}}{dE_1 d\Omega_1 d\Omega_2} \propto \frac{1}{4\pi} \int d\Omega \left| \left\langle \boldsymbol{p}\Psi_f^{N-1} \middle| \Psi_i^N \right\rangle \right|^2. \tag{4}$$

Here $\boldsymbol{p}$ is a plane wave representing the target electron at the collision instant, Ψ_i^N and Ψ_f^{N-1} are the target wave functions describing the N-electron initial neutral and $(N-1)$-electron final ionic states, respectively, and $\frac{1}{4\pi}\int d\Omega$ is the spherical averaging due to the random orientation of gaseous targets. The structure factor $\langle \boldsymbol{p}\Psi_f^{N-1}|\Psi_i^N\rangle$ in Eq. (4) is often described as

$$\left\langle \boldsymbol{p}\Psi_f^{N-1} \middle| \Psi_i^N \right\rangle = \sqrt{S_\alpha^f}\,\psi_\alpha(\boldsymbol{p}). \tag{5}$$

Here $\psi_\alpha(\boldsymbol{p})$ is the momentum-space representation of the quasiparticle or Dyson orbital and S_α^f is a quantity called pole strength. In the present study, the Dyson orbitals, their binding

energies, and pole strength values were calculated by using the symmetry adapted cluster configuration-interaction (SACCI) method [20] with the 6-311G** basis set, implemented in GAUSSIAN 09 [21], while a molecular structure of C_s symmetry (staggered conformation) was considered for both the S_0 and S_1 states [22,23]. In the calculations, the energy distribution of pole strength was limited, due to the high computational cost, up to approximately 25 and 20 eV for ionization from the S_0 and S_1 states, respectively. The associated theoretical spectra were then obtained by assuming that each ionization transition had a Gaussian profile with a width of the instrumental energy resolution and by summing up their contributions.

It can be seen from Fig. 1(a) that the poor instrumental energy resolution only allows the spectral peaks to be identified as two broad bands centered at around 14 and 24 eV, which are a group of peaks due to the outer-valence and inner-valence ionization, respectively. It is also can be seen that the experiment is on the whole well reproduced by the theoretical spectrum over the entire binding energy range that the SACCI calculations covered. On the other hand, though the data statistics are low, there are two additional features of the S_1 spectrum in Fig. 1(b). One is the appearance of a very weak band at a lower-binding-energy region centered at 4–5 eV and the other is a shift of both the outer- and inner-valence bands towards higher energy by about 3 eV compared to those at ~14 and ~24 eV in the S_0 spectrum.

The appearance of a band at 4–5 eV in the S_1 spectrum is expected from consideration of energy conservation: Subtraction of the photon energy of the 267-nm pump laser (4.64 eV) from the first ionization potential for the toluene S_0 state (8.83 eV) [24] leads to 4.2 eV. The weak band intensity originates mainly in the electron occupation number. Namely, the present SACCI calculations indicate that the wave function of the toluene S_1 state can be approximated as a linear combination of two electronic configurations with nearly the same expansion coefficients, $0.70[(3\pi)^{-1}(1\pi^*)^1] + 0.63[(2\pi)^{-1}(2\pi^*)^1]$. Note here that the two $1\pi^*$ and $2\pi^*$ excited orbitals are almost equally occupied by one electron. Thus, the energetically close-lying transitions from the S_1 state to the ground ($D_0[(3\pi)^{-1}]$) and first excited ($D_1[(2\pi)^{-1}]$) states of the toluene cation, illustrated in Fig. 2, appear at 4–5 eV with small pole strength values similar to each other.

Another feature of the S_1 spectrum in Fig. 1(b), the 3-eV shift of the outer- and inner-valence bands towards higher energy, can be understood by considering the nature of the structure factor in Eq. (4). That is, one-electron processes are allowed as in the case of the transitions to the D_0 and D_1 states discussed above, but two-electron and other multielectron processes are all forbidden. For instance, consider the second excited state of the toluene cation ($D_2[(15\sigma)^{-1}]$). For this state, although the transition from the S_0 state is allowed, that from the S_1 state is forbidden, as it is a two-electron process. On the contrary, transitions from the S_0 state to higher-energy ionic states of two-hole–one-particle ($2h1p$) configurations $[(15\sigma)^{-1}(3\pi)^{-1}(1\pi^*)^1]$ and $[(15\sigma)^{-1}(2\pi)^{-1}(2\pi^*)^1]$ are forbidden, but those from the S_1 state are allowed. The same argument can be made for all other, more tightly bound molecular orbitals. Indeed, the present SACCI calculations indicate that such $2h1p$ configurations in the final ion states account for more than 73% of the sum of the pole strength

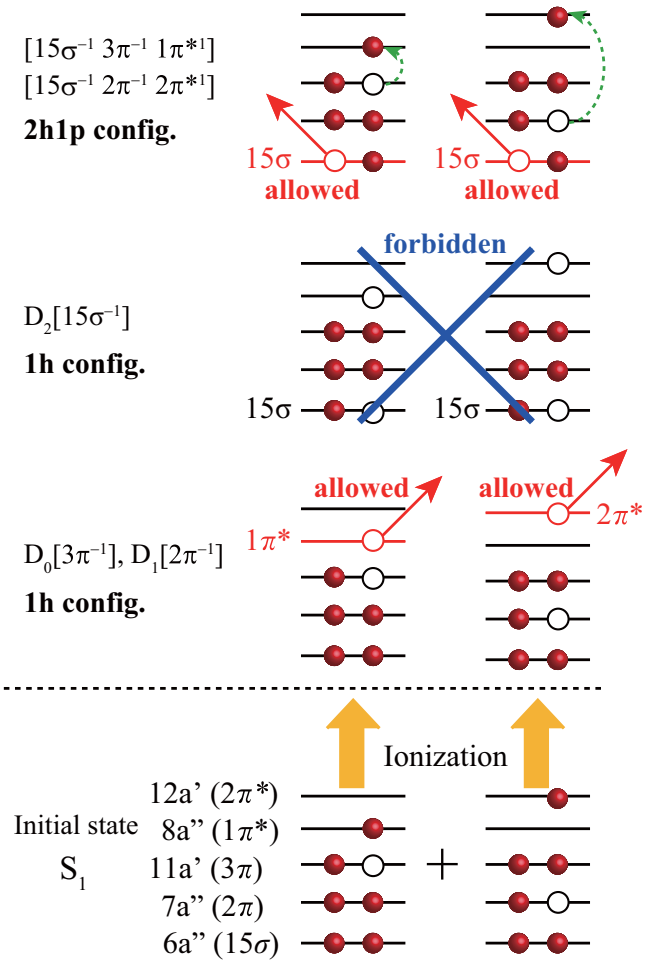

FIG. 2. EMS ionization schemes for transitions from the toluene S_1 state to several ionic states within the frozen orbital approximation, showing their occupation with electrons (closed circles) or holes (open circles).

values distributed over the considered binding energy range. Thus, the amount of the shift of the outer- and inner-valence bands towards higher energy can be approximated by the difference between the π-π^* excitation energies in the S_0 and D_0 states, i.e., $E^{D_0}_{\pi\pi^*} - E^{S_0}_{\pi\pi^*}$. The SACCI calculations predict 7.5 and 4.6 eV for $E^{D_0}_{\pi\pi^*}$ and $E^{S_0}_{\pi\pi^*}$, respectively, leading to the band shift energy of 2.9 eV, which is in good agreement with the experimental value of ~3 eV.

These observations discussed above may be eligible to extend the application of the propensity rule of EMS to molecular excited states as follows: The primary ionization process is the transition to the corresponding $1h$ configuration for the singly occupied molecular orbital of higher energy and to the $2h1p$ configurations for fully occupied orbitals as well as another singly occupied orbital of lower energy. Note that the critical role of $2h1p$ configurations is not a drawback of TREMS but an indication of its inherent capability to observe spatial distributions, in momentum space, of not only the outermost orbital but also all other, more tightly bound orbitals of a molecular excited state. This is because in primary ionization to such a $2h1p$ configuration the Dyson orbital is always of either the fully occupied orbitals or the

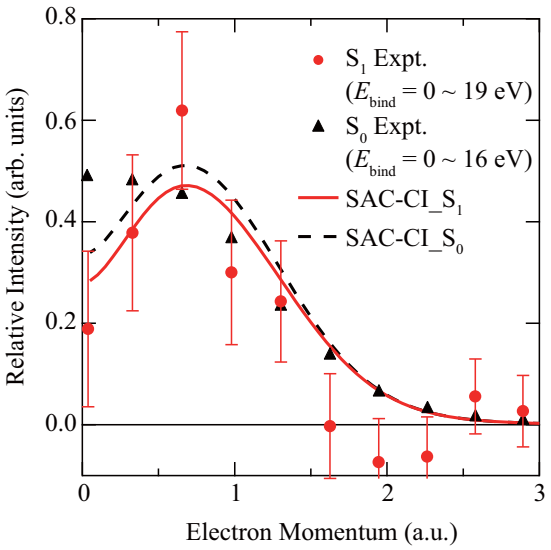

FIG. 3. Comparison of spherically averaged valence electron momentum distribution of the toluene S_1 state with that of the S_0 state as well as with the associated SACCI calculations.

singly occupied orbital of lower energy, which could be separately observed if the energy resolution were improved to the desired extent. This aspect is further strengthened by a unique advantage of EMS that a satellite band exhibits an electron momentum distribution similar in shape to that of its primary ionization band [3–6].

Finally, the spherically averaged electron momentum distribution measured for the outer valence orbitals of the toluene S_1 state is presented in Fig. 3 and compared with that of the S_0 state. They were obtained by plotting the number of true coincidence events that formed the outer-valence bands ($E_{\text{bind}} < 16$ and 19 eV for the S_0 and S_1 spectra in Fig. 1) as a function of the electron momentum p. Also included in the figure are the associated SACCI calculations, which were folded with the instrumental momentum resolution according to the procedure of Migdall *et al.* [25]. There are small but significant differences in both intensity and shape between the two theoretical distributions. We believe the principal source of the differences is effects of the $\pi - \pi^*$ electronic excitation rather than missing poles (< 0.01) in the theoretical calculations. The experimental results are then each area normalized to the corresponding theoretical ones.

It can be seen from Fig. 3 that though the S_0 theoretical distribution reproduces the experiment qualitatively, theory moderately underestimates and overestimates the experimental intensities at $p \sim 0$ a.u. and medium momenta (approximately 0.6–1.2 a.u.). A similar observation was made for the Ne $2s$ and $2p$ orbitals when the pulsed electron beam was used [12], while satisfactory agreement between experiment and theory has been known to be achieved for the Ne $2s$ and $2p$ orbitals by traditional EMS studies that employed a continuous incident electron beam [3–6]. Thus this observation would indicate the need for the development of an appropriate momentum resolution folding procedure, since the telefocus property of the pulsed electron beam may have been lowered, compared to that employed in traditional EMS studies, by possible, nonuniform angular spread due to the nonuse of an electrostatic lens system as well as by the use of the exceptionally large diameter (2 mm). On the other hand, interestingly, the tendency of the difference between the S_1 experimental and theoretical results appears to be opposite at $p \sim 0$ a.u.: Theory appears to overestimate the experimental intensity. This observation cannot be attributed to the insufficient treatment of the momentum resolution folding, because the S_1 and S_0 experimental data were concurrently obtained under the completely same conditions. Thus, if the observations are real, they would indicate the need for theoretical improvements in terms of a spatial distribution in describing the wave function of the toluene S_1 excited state. This is particularly so for its large-r part that is of central importance in the understanding of reactivity and molecular recognition, as a high electron density at large r leads to a high density at small p and vice versa by the nature of the Fourier transform. However, poor statistics of the S_1 experimental result make it difficult to discuss a change of the electron distribution due to electronic excitation; hence we leave the issue for later experiments with improved data.

In short, the present work reported the TREMS experiment on the toluene S_1 excited state with a lifetime of 86 ns. The ionization propensity rule has been extended through comparisons between the experimental and SACCI binding energy spectra, elucidating the inherent capability of TREMS to observe spatial distributions, in momentum space, of not only the outermost orbital but also all other, more tightly bound orbitals of a molecular excited state. In addition, the valence electron momentum distribution of the S_1 state was compared with that of the S_0 state as well as with theory, raising a fundamental issue as to how valence orbitals are changed in shape as a whole upon electronic excitation.

This work was partially supported by Scientific Research Grants (No. 20225001, No. 25248002, No. 15H03762, and No. 15K13615) from the MEXT of Japan. It was also supported in part by the Management Expenses Grants for National Universities Cooperation and the Yamada Science Foundation.

[1] F. Wilkinson, *Chemical Kinetics and Reaction Mechanisms* (Van Nostrand Reinhold, New York, 1981).
[2] K. Fukui, Science **218**, 747 (1982).
[3] E. Weigold and I. E. McCarthy, *Electron Momentum Spectroscopy* (Kluwer Academic/Plenum, New York, 1999), and references therein.
[4] K. T. Leung and C. E. Brion, J. Electron Spectrosc. Relat. Phenom. **35**, 327 (1985).
[5] M. A. Coplan, J. H. Moore, and J. P. Doering, Rev. Mod. Phys. **66**, 985 (1994).
[6] M. Takahashi, Bull. Chem. Soc. Jpn. **82**, 751 (2009).
[7] J. M. Zuo, M. Kim, M. O'Keeffe, and J. C. H. Spence, Nature (London) **401**, 49 (1999).

[8] J. I. Pascual, J. Gómez-Herrero, C. Rogero, A. M. Baró, D. Sánchez-Portal, E. Artacho, P. Ordejón, and J. M. Soler, Chem. Phys. Lett. **321**, 78 (2000).
[9] J. Itatani, J. Levesque, D. Zeidler, H. Niikura, H. Pépin, J. C. Kieffer, P. B. Corkum, and D. M. Villeneuve, Nature (London) **432**, 867 (2004).
[10] P. Puschnig, S. Berkebile, A. J. Fleming, G. Koller, K. Emtsev, T. Seyller, J. D. Riley, C. Ambrosch-Draxl, F. P. Netzer, and M. G. Ramsey, Science **326**, 702 (2009).
[11] Y. Zheng, I. E. McCarthy, E. Weigold, and D. Zhang, Phys. Rev. Lett. **64**, 1358 (1990).
[12] M. Yamazaki, Y. Kasai, K. Oishi, H. Nakazawa, and M. Takahashi, Rev. Sci. Instrum. **84**, 063105 (2013).
[13] M. Yamazaki, K. Oishi, H. Nakazawa, C. Y. Zhu, and M. Takahashi, Phys. Rev. Lett. **114**, 103005 (2015).
[14] J. C. Owrutsky and A. P. Baronavski, J. Chem. Phys. **110**, 11206 (1999).
[15] T. Wogan, Physics **8**, 23 (2015).
[16] Research Highlights, Chemistry: Imaging of excited electron orbitals, Nature (London) **519**, 392 (2015).
[17] C. G. Hickman, J. R. Gascooke, and W. D. Lawrance, J. Chem. Phys. **104**, 4887 (1996).
[18] *Modern Trend in Chemical Reaction Dynamics: Experiment and Theory, Part II*, edited by X. Yan and K. Liu (World Scientific, Singapore, 2004).
[19] B. J. Siwick, J. R. Dwyer, R. E. Jordan, and R. J. D. Miller, J. Appl. Phys. **92**, 1643 (2002).
[20] H. Nakatsuji, Chem. Phys. Lett. **177**, 331 (1991).
[21] M. J. Frisch *et al.*, GAUSSIAN 09, Revision D.01 (Gaussian, Inc., Wallingford, 2013).
[22] D. R. Borst and D. W. Pratt, J. Chem. Phys. **113**, 3658 (2000).
[23] C. Serralheiro, D. Duflot, F. Ferreira da Silva, S. V. Hoffmann, N. C. Jones, N. J. Mason, B. Mendes, and P. Limão-Vieira, J. Phys. Chem. A **119**, 9059 (2015).
[24] K. Kimura, S. Katsumata, Y. Achiba, T. Yamazaki, and S. Iwata, *Handbook of HeI Photoelectron Spectra of Fundamental Organic Molecules* (Halsted, New York, 1981).
[25] J. N. Migdall, M. A. Coplan, D. S. Hench, J. H. Moore, J. A. Tossell, V. H. Smith, Jr., and J. W. Liu, Chem. Phys. **57**, 141 (1981).